Reevaluating Cell Wraparound Techniques for 3D Channel Model based System-level Simulations

Ananth V. Kini, Mohsen Hosseinian, Moon-il Lee, Janet Stern-Berkowitz
{ananth.kini, mohsen.hosseinian, moonil.lee, janet.stern}@interdigital.com
InterDigital, Inc., USA

***Abstract*— Current wireless system-level simulation frameworks utilize cell wraparound in order to reduce boundary effects and provide an accurate evaluation of system performance. The current wraparound technique is purely distance based, where UEs always pick the closest cells, ignoring the radio propagation characteristics of the channel. While this wraparound methodology works well for a 2D channel model, it fails to account for the enhancements and spatial characteristics of the 3D channel model. In this paper we investigate the use of a radio distance based wraparound scheme for 3D channel models. This new wraparound methodology uses received downlink signal power to perform wraparound cell selection, allowing it to account for the radio propagation characteristics of the 3D channel model. We compare the performance of these two wraparound techniques with respect to coupling gain and other key metrics when considering a 3D channel model. Our results demonstrate the differences between the two schemes and highlight the improved accuracy offered by the radio distance based wraparound scheme.**

I. Introduction

In Third Generation Partnership Project (3GPP) based cellular systems, all cells may utilize the same channels. As a result, every cell may interfere with every other cell in the network. In order to realistically capture the interference encountered in a cellular system, one needs to model the layout of the system as accurately as possible. From a system-level simulation standpoint, this entails utilizing a network deployment that minimizes boundary effects while keeping system complexity in check. Various wireless and 3GPP based system level simulation frameworks use cell wraparound [1], [2] for minimizing the boundary effects. Consider a single operator deployment consisting of 19 cell sites with 3 sectors per site. This 19 site deployment is categorized as a cluster. Cell wraparound looks to emulate an infinite network by considering an extended network that includes additional shifted versions of this 19 site cluster. To be more precise, cell wraparound adds additional clusters of cells around a central cluster for a total of 7 clusters (the central cluster and 6 replicas shifted in location to the boundaries of the central cluster). Fig. 1 depicts the cell wraparound technique described above. The sites in the central cluster are numbered $1-19$ and each site has 3 sectors. A red circle indicates the location of each 3-sector site. The shifted replicas of the central cluster are denoted by sites $20-38, 39-57, 58-76, 77-95, 96-114$, and $115-133$, respectively. UEs are always dropped in the central cluster only. At the start of the simulation, for the purpose of link evaluation, each UE will select the closest version of each of the 19 sites from all 7 clusters based on Euclidean distance. For simplicity of discussion, we consider all versions of the clusters to be replicas, including the central cluster. As an example, consider a UE that is initially dropped in site 14 and looking to select the closest replica of site 10. It will choose from among all 7 replicas $(10, 29, 48, 67, 86, 105, 124)$ of this site, selecting site 29 since it is the closest to site 14. This site and hence, the sectors within this site, will then be used when considering links between the UE and site 10. Since this cell wraparound technique is based purely on distance, it can also be referred to as geographical distance based wraparound.

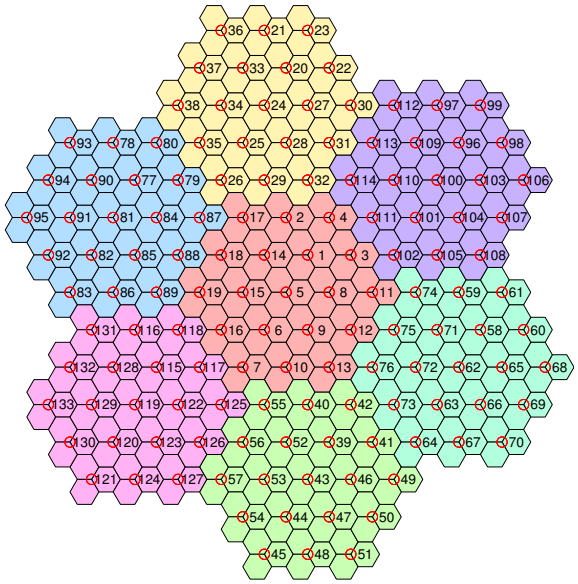

Fig. 1. Illustration of cell wraparound utilized in 3GPP system-level simulation frameworks. Cell sites (each with 3 sectors) are denoted by red circles. Each site cluster is depicted by a different color.

Although this wraparound technique works well for current system-level simulation frameworks, it suffers from certain limitations. Since a purely distance based wraparound approach ignores radio propagation characteristics such as antenna gain directivity at the eNB transmitter, the estimate of the received signal quality and interference may be overly optimistic or pessimistic. The geographical distance based approach also ignores any effects of elevation, which until recently have not been considered. The channel model used for system-level simulations in 3GPP based frameworks has been based on a geometry based stochastic model, which is a 2D channel model. For UEs dropped on the ground level, wraparound based on geographical distance may provide accurate enough results from a system-level simulation stand-

978-1-4799-8406-0/15/$31.00 ©2015 IEEE

point. As a result, this is the de facto methodology utilized when performing system level evaluations of cellular systems [3], [4]. An increasing interest in 3D channel models for Long Term Evolution (LTE) [5], however, has resulted in the need to reevaluate the accuracy of a geographical distance based wraparound approach. The main scenarios of interest for 3D channel model evaluations are based on dropping a significant percentage of UEs indoors and at a height of several floors. UEs on higher floors have a higher line of sight (LoS) probability and the pathloss experienced by a UE depends on this LoS probability. In the 3D model, a UE positioned indoors does not necessarily imply a high pathloss, especially for a UE located on a higher floor. Considering the differences in UE deployment for the 3D channel case and its potential effect on the radio propagation characteristics, one can expect to see a more noticeable difference in performance between an approach that does not account for radio propagation characteristics and one that does.

In this paper, we study two different wraparound methodologies: the traditional geographical distance based wraparound scheme, and a new radio distance based wraparound scheme. While geographical distance based wraparound selects the closest replica of each of 19 sites, radio distance based wraparound uses the received signal power to select the strongest replica of each of 57 sectors.

The rest of the paper is organized as follows: the 3D channel model is discussed in Section II; geographical and radio distance based wraparound are compared in Section III; simulation results are provided in Section IV; finally a conclusion is made in Section V.

II. Channel Model

Channel modeling plays a key role in accurately evaluating the performance of a wireless system. When standardizing wireless systems, it is especially important to be able to calibrate performance across a common set of reference channel scenarios. Existing channel models are generally two dimensional, meaning that wave propagation only considers azimuth angles. 3D channel models consider wave propagation in both azimuth and elevation directions, thereby providing an additional degree of freedom.

3D channel modeling has been discussed in WINNER II [6] and WINNER+ [7] projects, and [6] provides an outline of the steps required to extend the WINNER II model to a 3D one. The 3D channel model used in this paper is based on extensions of the 3GPP 2D channel model [8]. For a detailed description of the modifications required to extend the 2D channel to a 3D channel, as well as the validation of the 3D channel used in this paper, we refer the reader to [9].

UE Deployment Based Channel Characteristics

The focus of this paper is on investigating the effects of using geographical distance vs. radio distance based wraparound on UE serving cell selection (e.g., for attachment) and the relevant cell selection based metrics such as downlink SINR, coupling gain, etc., when performing system-level simulation. With this in mind, we focus our attention on various aspects of the 3D channel model and UE deployment that can influence UE serving cell (actually cell site sector) selection. In 3GPP LTE 3D Urban Macro (3D-UMa) and 3D Urban Micro (3D-UMi) scenarios using a 3D channel model, 80% of UEs are required to be dropped in buildings with a height between 10.5 m and 22.5 m [5], and an indoor UE can be located on any floor in a building where each floor is assumed to be 3.0 m high. Fig. 2 illustrates the various distance terms for such a deployment scenario. In this figure, $d_{3\mathrm{D-in}}$ and $d_{2\mathrm{D-in}}$ are indoor distances (distance from the UE to the interior wall) in m for UEs that are located inside a building, while $d_{3\mathrm{D}}$ and $d_{2\mathrm{D}}$ are the 3D and 2D distances (in m) from the base station (BS) to the exterior wall, where the BS is the physical transmission/reception location of the cell (or sector). For UEs dropped outdoors, we no longer have indoor distances, and $d_{3\mathrm{D}}$ and $d_{2\mathrm{D}}$ are the 3D and 2D distances (in m) from the BS to the UE. Antenna downtilts for the 2D and 3D channels are represented by $\theta^{2\mathrm{D}}_{\mathrm{etilt}}$ and $\theta^{3\mathrm{D}}_{\mathrm{etilt}}$, respectively.

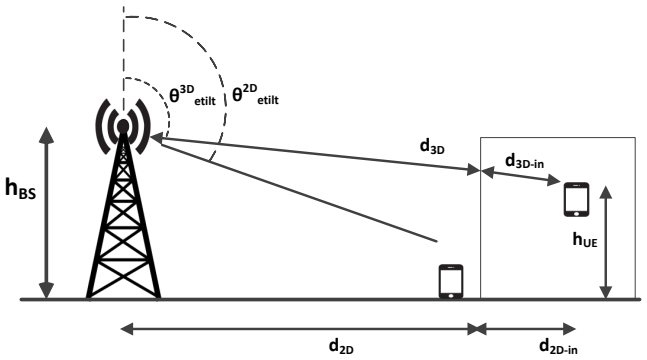

Fig. 2. 2D and 3D distances associated with 3D channel based UE dropping scenarios. Also illustrated are the antenna downtilts for the 2D and the 3D channel cases.

The LoS probability for the 2D-UMa case is given by (Table 4.7 in [6]):

$$P_{\mathrm{LoS}}^{\mathrm{2D-UMa}} = \\ (\min(18/d_{2D}, 1) \times (1 - \exp(-d_{2\mathrm{D}}/63)) + \exp(-d_{2\mathrm{D}}/63)), \quad (1)$$

and depends only on $d_{2\mathrm{D}}$, the distance from the BS to the exterior wall.

The LoS probability for the 3D-UMa channel scenario is given by (Table 7.2-2 in [5]):

$$P_{\mathrm{LoS}}^{\mathrm{3D-UMa}} = \\ (\min(18/d_{2\mathrm{D}}, 1) \times (1 - \exp(-d_{2\mathrm{D}}/63)) + \exp(-d_{2\mathrm{D}}/63)) \\ \times (1 + C(d_{2\mathrm{D}}, h_{\mathrm{UE}})), \quad (2)$$

where $d_{2\mathrm{D}}$ is (as above) the distance from the BS to the exterior wall, h_{UE} is the UE antenna height, and $C(d_{2\mathrm{D}}, h_{\mathrm{UE}})$ and $g(d_{2\mathrm{D}})$ are given by:

$$C(d_{2\mathrm{D}}, h_{\mathrm{UE}}) = \begin{cases} 0, & h_{\mathrm{UE}} < 13 \text{ m} \\ (\frac{h_{\mathrm{UE}}-13}{10})^{1.5} \times g(d_{2\mathrm{D}}), & 13 \le h_{\mathrm{UE}} \le 23 \text{ m} \end{cases} \quad (3)$$

and

$$g(d_{2\mathrm{D}}) = \begin{cases} 1.25 \times 10^{-6} \times d_{2\mathrm{D}}^3 \times exp(-\frac{d_{2\mathrm{D}}}{150}), & d_{2\mathrm{D}} > 18 \text{ m} \\ 0, & \text{otherwise.} \end{cases} \quad (4)$$

From Eqns (2) to (4) we observe that, for the 3D-UMa scenario, the LoS probability depends on the UE height; from Eq (1), we can see this is not the case for 2D-UMa. This LoS probability has a direct impact on the pathloss experienced by a UE (Table 7.2.1 in [5]) and therefore UE height impacts pathloss. Effectively, in the 3D channel case, an indoor UE that is far away from a BS (large d_{2D}) has a higher probability of LoS (and potentially lower pathloss) to this BS if it is at a favorable height (h_{UE}); this is not considered by the geographical distance based wraparound approach. Furthermore, the pathloss experienced by a UE at a given height can be affected by antenna downtilt. The intent of the downtilt angle is for the downtilt vertical beam to reduce inter-cell interference while increasing antenna gain for the UEs served in the cell. Unlike the 3GPP 2D channel model which uses a fixed antenna downtilt and is intended for UEs which are all dropped at ground level, the antenna downtilt for the 3D channel model can be adapted per BS (e.g., based on UE distribution). If the downtilt angle of a faraway BS is reduced to increase antenna gain for indoor UEs located on higher floors (e.g., as shown in Fig. 2), an indoor UE may experience a lower pathloss and hence a stronger received signal to this BS in comparison to another BS that is closer. As a result, the best BS for a UE may be one that is further away, something the purely geographical distance based wraparound approach would not be able to account for.

We now take a closer look at the difference between the geographical and radio distance based wraparound approaches with respect to serving cell (i.e., sector) selection.

III. Geographical Distance vs. Radio Distance Based Wraparound

As mentioned earlier, the geographic wraparound technique selects sites based on Euclidean distance. This site based selection results in selection of sectors within the same replica for that particular site. Fig. 3 illustrates how this technique works.

In the figure, the sites located in the central replica are in blue, whereas the shifted replica sites are in red. UEs are dropped in the central replica and, for each UE, the closest replica of each of the 19 sites is chosen. Consider a UE dropped in the central replica (near site $A1$). In order to find the closest replicas for the 19 sites, we calculate the distance from this UE to all seven replicas of each site. As an example, consider site $A1$ with wraparound replicas $B1, C1, D1, E1, F1, G1$. In this case, it is obvious that site $A1$ is the closest to the UE and will be picked while the various wraparound replicas are discarded. Consider now site $A2$ with wraparound replicas $B2, C2, D2, E2, F2, G2$. In this case, we see that when considering the link between the UE and site $A2$, we need to consider the wraparound replica $C2$ (circled) of this site, as this is the one that is closest to the UE. Each of the 19 chosen sites has 3 sectors associated with it, for a total of 57 sectors. For its serving cell, the UE will choose the sector (from the 57 sectors) with the strongest reference signal received power (RSRP) [10].

In radio distance based wraparound, each *sector* (as opposed to each *site* in the geographical distance wraparound scheme) is selected on the basis of received downlink signal power

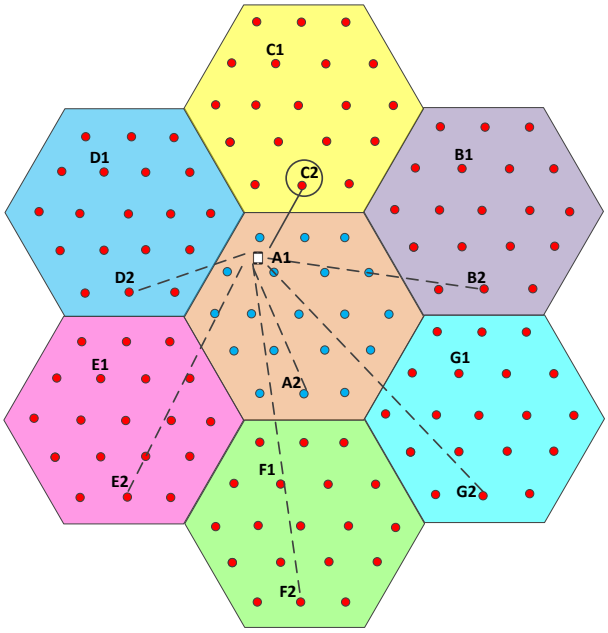

Fig. 3. Illustration of geographical distance based wraparound.

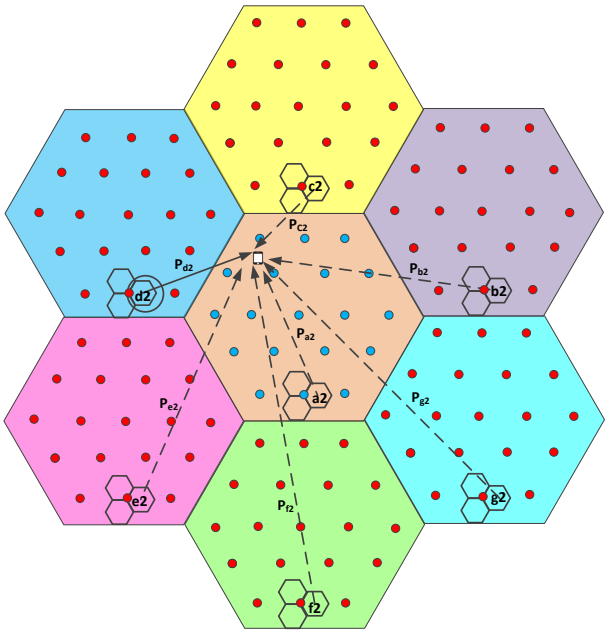

Fig. 4. Illustration of radio distance based wraparound.

(using RSRP) from all seven replicas of that sector. Since sectors are selected individually, the sectors for a given site may be chosen from different replicas of that site. Fig. 4 illustrates the sector selection process. We focus on sector $a2$ and its wraparound replicas. For the radio distance wraparound scheme, the RSRP (denoted by P) from all seven replicas of this sector ($a2, b2, c2, d2, e2, f2, g2$) are used to select the replica with the strongest RSRP. In this figure, we assume sector d_2 (circled) has the strongest RSRP at the UE and, hence, is the one that will be selected. This will then be used when considering the sector-to-UE links for $a2$. After repeating the process for each sector, the result is again 57 sectors from which the UE will choose the one with the strongest RSRP for its serving cell.

One of the main differences between these two wraparound schemes is the fact that the geographical distance scheme starts by picking 19 sites (out of $19 \times 7 = 133$) in the first step. After this initial site selection process, the RSRP from each of the $19 \times 3 = 57$ sectors of those 19 sites is then computed for the UE serving cell selection stage; this does not guarantee selection of the sector with the highest RSRP. By contrast, in the radio distance scheme, the initial sector selection itself is based on RSRP from all seven replicas of each sector, ensuring attachment to the sector with the highest RSRP; this is more representative of true system behavior. The downside of this method is that it requires calculation of RSRP for $57 \times 7 = 399$ sectors, resulting in a seven fold increase in RSRP computation at the start of each simulation run.

Since the radio distance based approach clearly provides more realistic behavior, the question becomes whether the added computational complexity and simulation time is warranted, or if the geographic distance based method is good enough. In the following section, we present simulation results comparing the two schemes in a 3D system with respect to estimates of various metrics such as SINR and coupling gain to demonstrate the improvements which can be achieved by the radio distance based approach. Measurable differences between the two schemes translate into more accurate estimates when using the radio distance scheme over the geographic distance scheme.

IV. Simulation Results

We consider a 19 macro site deployment with 3 sectors per site. We simulate both wraparound techniques in order to compare their performances. Each sector has 10 dropped UEs for a total of 570 UEs in the system. We consider two different rectangular antenna array configurations for the purpose of this evaluation, (i) $K = M = 1$, with $N = 2$ and (ii) $K = M = 10$, with $N = 2$. Here N denotes the number of antenna columns, M denotes the number of antenna elements per column and K specifies the number of antenna elements per port. For $K = M = 10$, the 10 vertical elements are formed into one antenna port with a beamforming weight for electrical downtilt (etilt). We consider both 3D-UMa and 3D-UMi scenarios for this evaluation. Details for these scenarios as well as UE dropping specifics can be found in [5]. Additional system level simulation parameters relevant to our study are provided in Table I.

TABLE I
System level simulation parameters

Parameter	**Value**
System bandwidth	10 MHz (50 RBs)
Frequency	2 GHz
Duplex	FDD
Scenarios	3D-UMa, 3D-UMi
BS antenna configs.	Config. 1: $K = M = 1, N = 2$, ULA, 0.5λ H/V spacing Config. 2: $K = M = 10, N = 2$, X-pol $(+/-45)$, 0.5λ H/V, $\theta_{etilt} = 96°$
MS antenna configs.	Config. 1: 2 Rx ULA, 0.5λ H spacing Config. 2: 2 Rx X-pol $(0/+90)$
Number of UEs per sector	10
Number of drops	10
UE attachment	Based on RSRP (formula) from CRS port 0 [11]
UE distribution	Follows TR 36.873 3D-UMa, 3D-UMi
UE speed	3km/h
UE array orientation	$\Omega_{UT,a}$ uniform dist. on $[0, 360]°$, $\Omega_{UT,b} = 90°, \Omega_{UT,g} = 0°$
UE antenna pattern	Isotropic ant. gain pattern $A'(\theta', \phi') = 1$
Wraparound method	1. Geographic distance 2. Radio distance
Cluster elimination step 6	Scaling factor not changed after cluster elimination
Handover margin	0 dB

We compare the two wraparound schemes on the basis of three different metrics: (i) coupling gain defined as the distance based gain (including shadowing, antenna gain, and penetration losses) between the antennas of the UE and its selected serving cell, (ii) wideband SINR defined as the downlink SINR for each UE based only on large scale parameters, i.e., without fast fading, and (iii) the distance to the selected serving cell for each UE.

Results

Fig. 5 (3D-UMa) and Fig. 6 (3D-UMi) plot the CDF of the coupling gain of UEs to their serving cells for $K = M = 1$ and $K = M = 10$ for both geographical and radio distance based wraparound schemes. For both 3D-UMa and 3D-UMi scenarios, we observe a difference in UE to selected serving cell coupling gain between the two wraparound schemes. This difference is more noticeable for low values of coupling gain where the difference is up to 3 dB for the 3D-UMa scenario, and up to 5 dB for the 3D-UMi scenario for $K = M = 1$. This holds true across all antenna configurations and can be explained by observing that in the geographical distance case, the UE may select a cell that is closer but perhaps does not have the best coupling gain. However, in the radio distance case, the initial serving cell selection itself is based on coupling gain, guaranteeing that the selected serving cell for each UE is the one that provides the best coupling gain. The difference between the two wraparound schemes decreases as we go from $K = M = 1$ to $K = M = 10$ and also as we move to the higher coupling gain region of the plots. The explanation is likely that the differences are more pronounced for the cases where the radio distance scheme is more able to take advantage of UE height, such as in the low coupling gain case where the BS is more likely to be far away, and the lower antenna tilt case, which can provide better pathloss to UEs at favorable height.

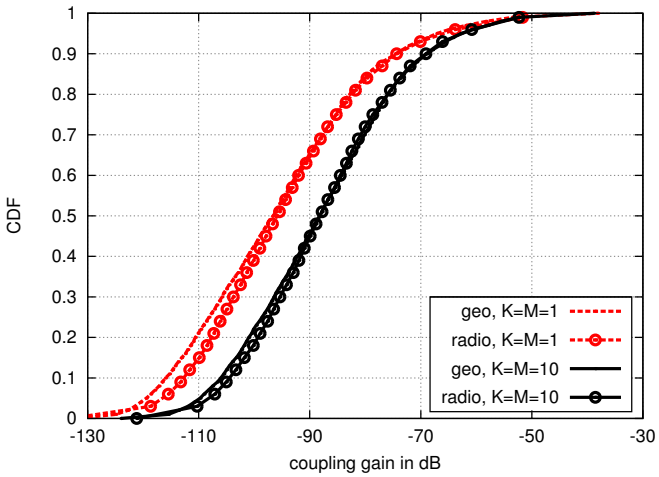

Fig. 5. CDF of coupling gain for geographical and radio distance based wraparound schemes for the 3D-UMa scenario with various antenna configurations.

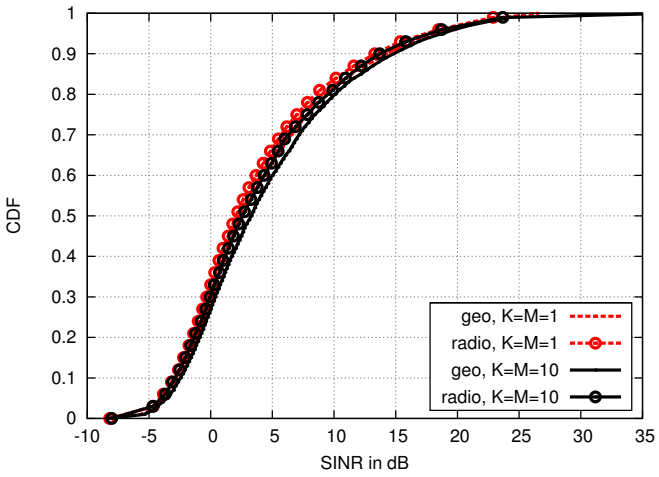

Fig. 7. CDF of downlink SINR for geographical and radio distance based wraparound schemes for the 3D-UMa scenario with various antenna configurations.

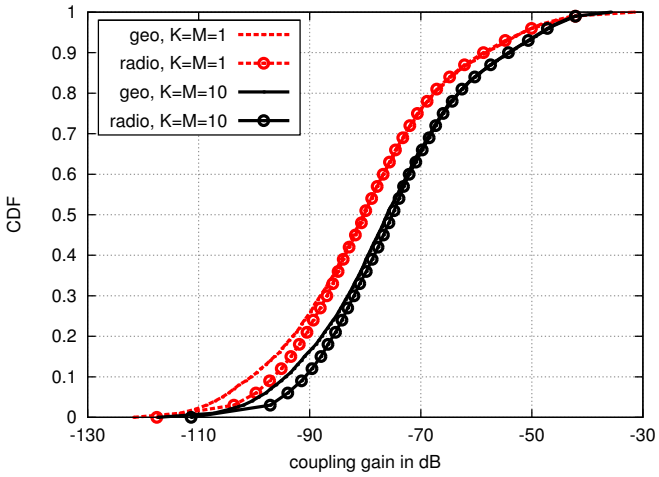

Fig. 6. CDF of coupling gain for geographical and radio distance based wraparound schemes for the 3D-UMi scenario with various antenna configurations.

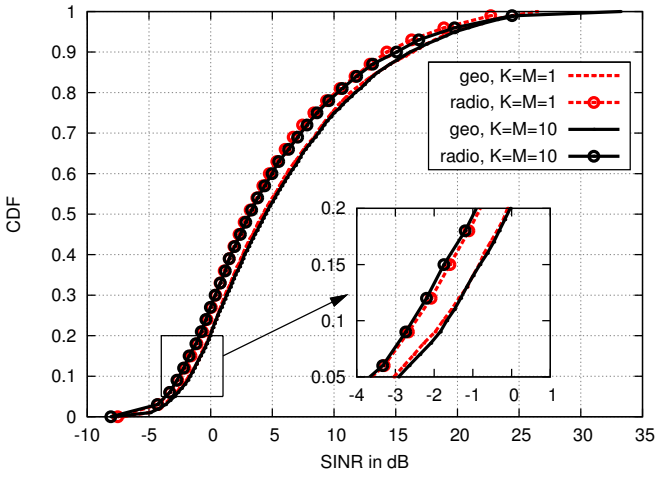

Fig. 8. CDF of downlink SINR for geographical and radio distance based wraparound schemes for the 3D-UMi scenario with various antenna configurations.

Fig. 7 (3D-UMa) and Fig. 8 (3D-UMi) plot the CDF of wideband SINR for $K = M = 1$ and $K = M = 10$ for both geographical and radio distance based wraparound schemes. We observe some difference in wideband SINR between the two wraparound schemes across all antenna configurations and for both 3D-UMa and 3D-UMi scenarios. This can be explained by looking into the cell selection process for the radio distance based wraparound scheme. Since radio distance based wraparound picks the strongest 57 cells (i.e., sectors), based on coupling gain/RSRP, both the serving as well as interfering cells are the strongest 57 out of 399 cells. Picking the strongest interfering cells in turn results in lower SINR. For the geographic wraparound scheme, the initial distance based selection of the 57 cells can result in the selection of cells that do not necessarily have the best RSRP. As a result, we may be underestimating the interference in the system, which in turn yields higher values of SINR. This difference is more noticeable for the 3D-UMi scenario. Focusing in particular on the low SINR (< 0 dB) region, we observe a difference of ≈ 1 dB in SINR between the geographic and radio distance based wraparound schemes. Overestimating the SINR may result in an overly optimistic estimate of throughput for the low SINR UEs, providing an inaccurate measure of true system performance.

Fig. 9 (3D-UMa) and Fig. 10 (3D-UMi) plot the CDF of distance to selected serving cell for $K = M = 1$ and $K = M = 10$ for both geographical and radio distance based wraparound schemes. We observe that the distribution of UE to serving cell distances across all antenna configurations and within each wraparound scheme is fairly similar for those UEs that are close to their serving cell (within 200 m or so for the 3D-UMa scenario and within 100 m or so for the 3D-UMi scenario). The common thread across all antenna configurations is the fact that UEs are more likely to pick serving cells that are further away in the radio distance based wraparound scheme, which is why we observe UEs with serving cells up to 4000 m and 1500 m away for 3D-UMa and 3D-UMi scenarios, respectively, for radio distance based wraparound as opposed to only 1300 m and 500 m away for geographical distance based wraparound.

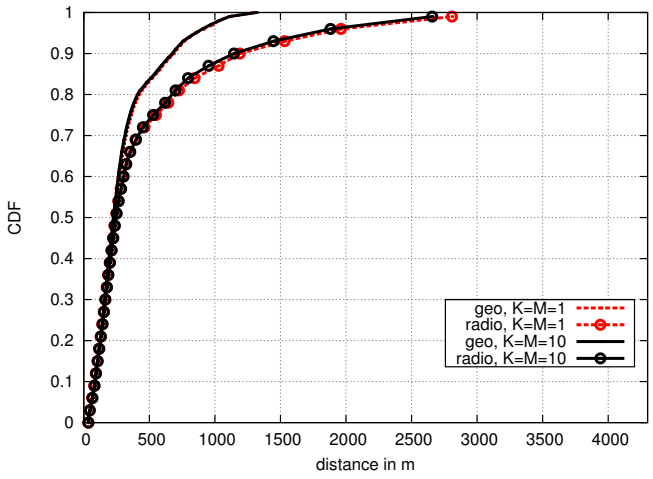

Fig. 9. CDF of distance to selected serving cell for geographical and radio distance based wraparound schemes for the 3D-UMa scenario with various antenna configurations.

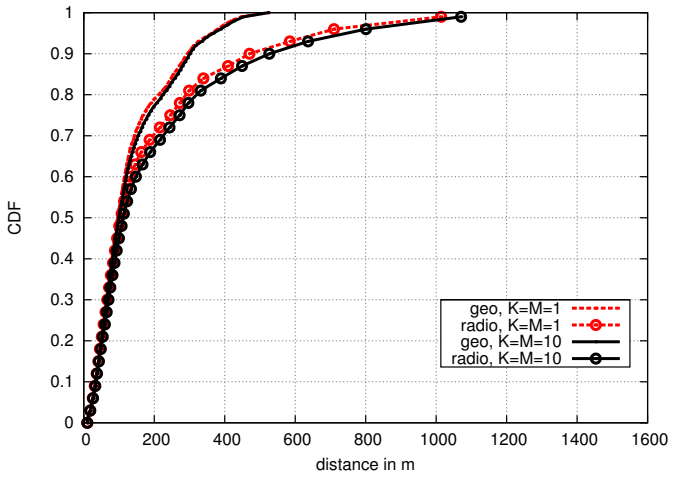

Fig. 10. CDF of distance to selected serving cell for geographical and radio distance based wraparound schemes for the 3D-UMi scenario with various antenna configurations.

Overall, our simulation results highlight the fact that there are measurable differences in key system metrics between the geographical distance and radio distance based wraparound schemes for 3D channel scenarios. These differences are a direct result of the cell selection methodologies used by these two wraparound schemes and the effect that UE height and BS antenna tilt can have on pathloss in a 3D system. Therefore, even though adopting a radio distance based wrapping scheme would result in an increase in computational complexity, we strongly recommend its use in order to provide a more accurate representation of the system-level performance for frameworks that utilize 3D channel models.

V. Conclusion

We evaluated the performance of geographical distance and radio distance based cell wraparound schemes for 3D channel models. In radio distance based wraparound, each sector is selected on the basis of received signal power from all replicas of that sector. In contrast, geographic distance based wraparound selects sites based on distance, not accounting for radio propagation characteristics. Our analysis and results demonstrate that the radio distance based approach allows for a more accurate representation of the various system-level simulation calibration metrics such as wideband SINR and coupling gain, which in turn can provide a better estimate of overall system performance. The trade-off when compared to a geographical distance based scheme, however, is an increase in RSRP computation complexity. Based on our observations, in order to provide a more accurate representation of system-level performance, we recommend use of the radio distance based wrapping methodology when using 3D channel model based system-level simulations.

References

[1] IEEE, "802.16m Evaluation Methodolody Document (EMD)," 2009.
[2] 3GPP TR 36.942, "Evolved Universal Terrestrial Radio Access: Radio Frequency RF System Scenarios (Release 12)," v12.0.0, 2014.
[3] A. Muller and P. Frank, "Cooperative Interference Prediction for Enhanced Link Adaptation in the 3GPP LTE Uplink," in *Vehicular Technology Conference (VTC 2010-Spring), 2010 IEEE 71st*, May 2010, pp. 1–5.
[4] C. Suh, M. Ho, and D. Tse, "Downlink Interference Alignment," *Communications, IEEE Transactions on*, vol. 59, no. 9, pp. 2616–2626, September 2011.
[5] 3GPP TR 36.873, "Study on 3D Channel Model for LTE (Release 12)," v12.0, 2014.
[6] P. Kyösti, "WINNER II Channel Models, d1.1.2 v1.1," 2007.
[7] J. Meinilä, "D.5.3: WINNER+ Final Channel Models, d1.1.2 v1.1," 2010.
[8] 3GPP TR 36.814, "Further Advancements for E-UTRA Physical Layer Aspects (Release 9)," v9.0.0, 2010.
[9] M. Jiang, M. Hosseinian, M. Lee, and J. Stern-Berkowitz, "3D Channel Model Extensions and Characteristics Study for Future Wireless Systems," in *Personal Indoor and Mobile Radio Communications (PIMRC), 2013 IEEE 24th International Symposium on*, Sept 2013, pp. 41–46.
[10] 3GPP TS 36.214, "Evolved Universal Terrestrial Radio Access (E-UTRA): Physical Layer Measurements (Release 12)," v12.1.0, 2014.
[11] 3GPP R1-136000, "RAN1 Working Group Meeting (Agenda item 6.2.7.2) - WF on RSRP Calculation," November 2013.